iJRASET
International Journal For Research in Applied Science and Engineering Technology

INTERNATIONAL JOURNAL FOR RESEARCH

IN APPLIED SCIENCE & ENGINEERING TECHNOLOGY

Volume: 6 **Issue:** I **Month of publication:** January 2018

DOI: http://doi.org/10.22214/ijraset.2018.1139

www.ijraset.com

Call: 08813907089 | E-mail ID: ijraset@gmail.com

International Journal for Research in Applied Science & Engineering Technology (IJRASET)
ISSN: 2321-9653; IC Value: 45.98; SJ Impact Factor:6.887
Volume 6 Issue I, January 2018- Available at www.ijraset.com

Effect of Super Cavitation Effect on AUV's

Goutham S[1], Pratap Kumar Panda[2], Naveen V Nair[3], Faiyaz Muhammad[4], T P Sreenath[5]
[1, 2, 3, 4, 5]*Mechanical Department, MG* University

Abstract**: Supercavitation phenomenon is that when an object moves in water and its speed increases constantly, according to Bernoulli's equation, this will make the hydrostatic pressure that it bears drop. And when the pressure down to the vaporization pressure of water at that temperature, the surface moisture of the object will change into steam, form bubbles and wrap it. Due to the density of water and steam has magnitude deviation, the viscous resistance acting on the underwater moving object will reduce greatly, that can make the performance of underwater weapon enhance markedly. In the military applications, there are represented by Russia, the torpedo of "snowstorm" used the ventilation supercavitation theory and, represented by USA, the "20mm Supercavitation projectile" used the nature supercavitation theory. As the nature of supercavitation projectile is a kind of remote controlled, rocket powered underwater weapon, the formation and stability of cavitation formed is more significant for performing the properties of projectile. This project focuses on numerical investigation for new designed supercavitation projectiles, focused on the cavitation morphology and various navigation cone stability under high velocity circumstance. For this numerical simulation unsteady Reynolds averaged Navier-Stokes equation is used. This research can provide sound basis for reasonable structure design of new projectiles.
Keywords: Supercavitation, projectile, AUV's

I. INTRODUCTION

This document is a template. For questions on paper guidelines, please contact us via e-mail.
Supercavitation is a hydrodynamic process in which an undersea body is almost entirely enveloped in a layer of gas initiated at a cavitator mounted at the forward end. A super cavity can be maintained in one of two ways: (1) by achieving such a high speed that the water vaporizes near the nose of the body; or, (2) by supplying gas to the cavity at nearly ambient pressure. The first technique is known as vaporous cavitation; the second is termed ventilation, or artificial cavitation.
Supercavitating bodies can achieve very high speeds under water by virtue of reduced drag: with proper design, a cavitation bubble is generated at the nose and skin friction drag is drastically reduced. Because the density and viscosity of the gas are dramatically lower than that of seawater, skin friction drag can be reduced significantly. If the body is shaped properly, the attendant pressure drag can be maintained at a very low value, so that the overall body drag is also reduced dramatically: by roughly eighty percent for a self-propelled vehicle capable of executing maneuvers, to an order of magnitude for free-flying gun-launched projectiles. However, because the centre of pressure is typically located well forward with respect to the center of gravity, control and maneuvering present special challenges. Also, whereas a fully wetted vehicle develops substantial lift in a turn due to vortex shedding off the hull, a supercavitating vehicle does not develop significant lift over the gas-enveloped surfaces. This requires a different approach to effecting hydrodynamic control.
For most of the last decade, the United States Navy has sponsored basic research and exploratory development programs addressing the physics and engineering of supercavitating high-speed bodies. This paper highlights some results of the Navy-sponsored activities at the Naval Undersea Warfare Center (NUWC).
An important element of the Navy program involves the development of theoretical and computational models that facilitate the investigation and understanding of the physics of supercavitating high-speed bodies. Such tools are also being incorporated into resources for simulating the behaviour of such systems, allowing assessment of their utility. Such simulations are expected to play an important role in planning experiments with free-running, self-propelled vehicles, in assessing the safety of such exercises, and in analyzing and applying test data.

II. LITERATURE REVIEW

To date, few experiments have been done on the topic of supercavitation. The experiment if carried out is often implemented by a solid object traveling underwater with a specific speed, and the movement of the solid object can initiate supercavitation depending on conditions associated with the flow surrounding the object. Cavitation and pressure distribution of different head forms at zero angle of yaw were investigated by Rouse and McNown (1948). But the speed of flow in their experiments was limited to less than 32m/s. On the basis of the potential flow theory, Brennen (1969) obtained numerical solutions for the cavity shapes and the drag

coefficients for blunt bodies in incompressible supercavitating flows. J. D. Hrubes (2001) employed various standard high speed imaging techniques to capture supercavitation in his experiment. Shockwaves were observed in supersonic underwater projectiles.
Vlasenko (2003) did some experimental investigations of supercavitation at subsonic and transonic speeds. In the experiment, the velocity was about 124m/s. Both results of the above experiments are still limited by the experimental equipment. As a result, numerical simulations have been gaining much popularity due to the rapid development in numerical methods as well as computing power. Numerical simulations are attractive because they can be used to study events closely related to the phenomena of supercavitating flow that are sometimes very difficult to observe experimentally owing to limitations in temporal and spatial resolution of experimental diagnostics. In addition, experimental work is also considerably more expensive than that of numerical simulations. Numerous investigations have been carried out with respect to cavitation over the past decades. Klomfass and Salk (2005) investigated using a 3D finite-volume approach of conservative equations were used to solve the inviscid compressible cavitating flow. However, the cavitation model used by Klomfass and Salk (2005) was limited to temperature sufficiently below the critical point. A preconditioned technique is applied to solve the full unsteady compressible Navier-Stokes equations by Owis and Nayfeh (2003). Based on the combination of time-derivative preconditioning strategies with low-diffusion upwinding methods.
Neaves and Edwards (2006) solved the Navier-Stokes equations as applied to the homogeneous mixture of fluids via a cell-centered finite-volume method to obtain the supercavitation. Both Owis and Nayfeh (2003) and Neaves and Edwards (2006) employ the preconditioned algorithm for the simulation which is quite complex to implement. ZengHuiming (2007) investigated supercavitation using two different solvers Eulerian solver modified Ghost Fluid Method. In his experimental analysis he used three different cavitation models, Cut-off model, isentropic model and one fluid cavitation model. The Eulerian solver and isentropic model of supercavitation successfully achieved stable supercavitation and also captured formation of cavitation around hemispherical nose body (Case 5.2.2) .
B. Saranjam (2013) used 6DOF schemes to study effect of supercavitation on spherical nose body. The domain had a deformable region sandwiched between 2 non deforming regions. In the experiment and simulation of unsteady supercavitation around a moving underwater body stable supercavitation at cavitation number 0.1 and below. PAN Shou-li and ZHOU Qiang (2014) employed Homogeneous Mixed Flow Theory for numerical setup of supercavitation around small body. They observed re-entrant jet was formed behind cavitation tail under the act of adverse pressure gradient; resistance coefficient was related to cavitation number, cavitation slenderness ratio and cavitator diameter. Based on the above literature survey the most researches favor numerical investigation, i.e., computational solving of supercavitation models. Thus, in our project CFD approach was chosen for analysis of supercavitation effect.

III.COMPUTATIONAL MODEL

A. Model geometries and grid generation.

Different model profiles have been considered, which includes cone nose and hemispherical nose. And the body with cylinder and aerodynamic profiles are combined with nose profiles. The model geometries are presented in Figs. 3.1a-3.2b. The three dimensional computation domain and grid distribution near one of the model are shown in Figs. 3.3 and 3.4, respectively. For ensuring computation accuracy, the mesh generation has been conducted carefully. The grid size is 352000 and 342000 for cone and hemi constant cylinder profile, 243000 and 222000 for cone and hemi aerodynamic profile respectively. The nose rear end diameter is 30 mm and cylinder diameter is 15mm. The model length is 150mm from end of the nose.

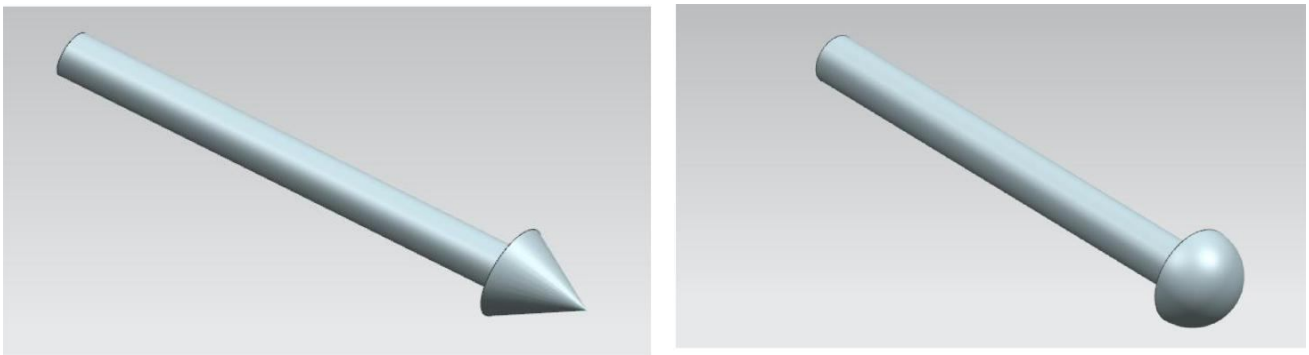

(A) (B)

ISSN: 2321-9653; IC Value: 45.98; SJ Impact Factor:6.887
Volume 6 Issue I, January 2018- Available at www.ijraset.com

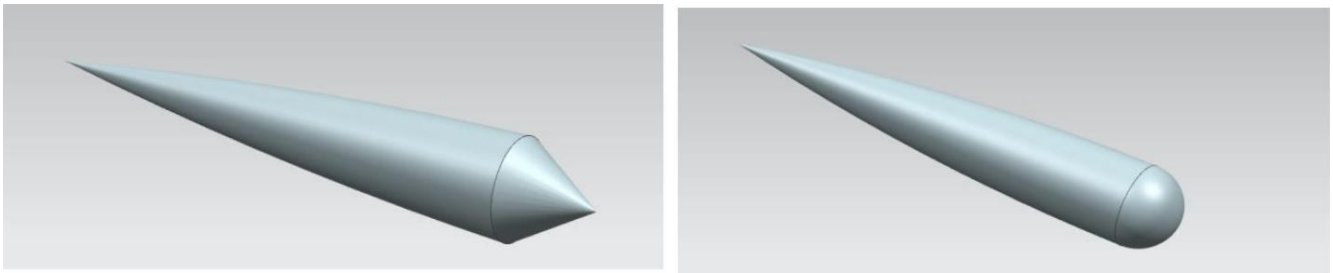

(C) (D)

Fig.1(A) Conical nose with cylinder profile. (B) Hemisherical nose with cylinder profile.(C) Conical nose with aerodynamic reducing profile. (D) Hemisperical nose with aerodynamic reducing profile

Domain is shaped as a cylinder to avoid unsymmetrical turbulence effects produced during fluid flow. Domain has a pressure inlet initially set to 30bar and pressure outlet is set to atmosphere. No outflow is expected out of the domain except at outlet. The length of the domain is 10m, with a min diameter of 1.2m. Angle of attack is 0˚.

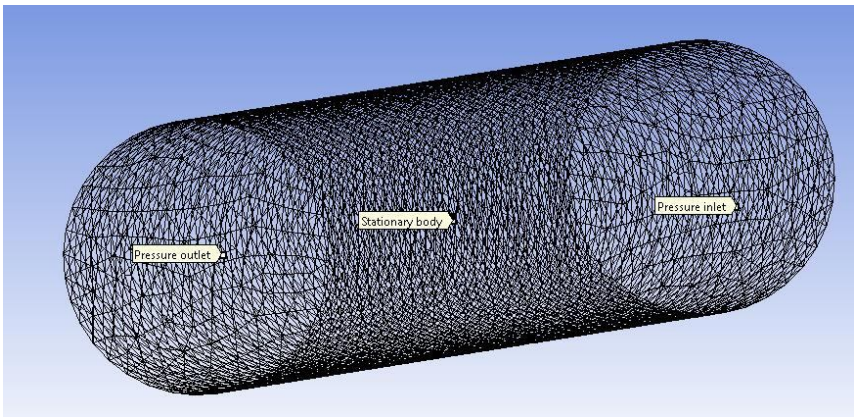

Fig. 2 The three dimensional computational domain and boundary conditions.

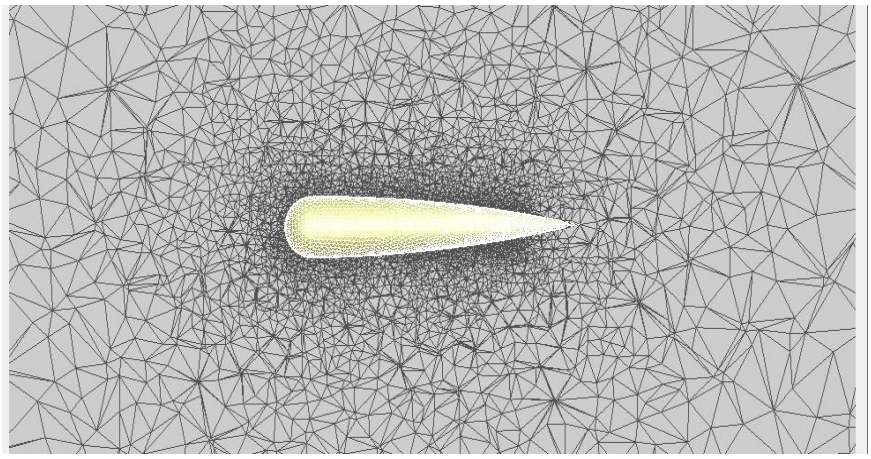

Fig. 2 The grid generated around the body.

B. Numerical model and fluid flow modeling.

The URANS dynamics model (unsteady Reynolds averaged Navier–Stokes equations) has been used as numerical method in order to simulate and predict unsteady cavitation shape, dynamics behaviour and acted forces on the bodies.

The Reynolds-averaged Navier–Stokes equations were solved for the supercavitating flow field in a computational domain based on the finite volume method and the pressure-based segregate algorithm, using mixture multiphase model.

The continuity equation for the mixture is [12]

$$\frac{\partial \rho_m}{\partial t} + \frac{\partial (\rho_m u_j)}{\partial x_j} = 0 \quad \ldots (1)$$

The momentum equations for the mixture is [12]

$$\frac{\partial}{\partial t}(\rho_m u_i) + \frac{\partial}{\partial x_j}(\rho_m u_i u_j) = -\frac{\partial p}{\partial x_i} + \frac{\partial}{\partial x_j}\left[(\mu_m + \mu_t)\left(\frac{\partial u_i}{\partial x_j} + \frac{\partial u_j}{\partial x_i}\right)\right] + \rho_m g_i \quad \ldots (2)$$

Where uj and xj represent the velocity component and the coordinate axis, respectively, t is the time, p denotes the local pressure, the density ρm and the viscosity μm of the mixture are computed in a volume–fraction–average manner, and μt indicates the turbulent viscosity.

The viscous equation set is closed by using the two equation realizable k-ε turbulence model.

Turbulent kinetic transport equation [12].

$$\frac{\partial}{\partial t}(\rho k) + \frac{\partial}{\partial x_j}(\rho k u_j) = \frac{\partial}{\partial x_j}\left[\left(\mu + \frac{\mu_t}{\sigma_k}\right)\frac{\partial k}{\partial x_j}\right] + G_k + G_b - \rho\varepsilon - Y_M + S_k \quad \ldots (3)$$

of dissipation of energy from the turbulent flow [12]:

$$\frac{\partial}{\partial t}(\rho\varepsilon) + \frac{\partial}{\partial x_j}(\rho\varepsilon u_j) = \frac{\partial}{\partial x_j}\left[\left(\mu + \frac{\mu_t}{\sigma_\varepsilon}\right)\frac{\partial \varepsilon}{\partial x_j}\right] + \rho C_1 S\varepsilon - \rho C_2 \frac{\varepsilon^2}{k + \sqrt{\nu\varepsilon}} + C_{1\varepsilon}\frac{\varepsilon}{k} C_{3\varepsilon} G_b + S_\varepsilon \quad \ldots (4)$$

where

$$C_1 = \max\left[0.43, \frac{\eta}{\eta + 5}\right], \quad \eta = S\frac{k}{\varepsilon}, \quad S = \sqrt{2 S_{ij} S_{ij}} \quad \ldots (5)$$

where the turbulent viscosity is

$$\mu_t = \rho C_\mu \frac{k^2}{\varepsilon} \quad \ldots (6)$$

The coefficient of dynamic viscosity is

$$C_\mu = \frac{1}{A_0 + A_s (kU/\varepsilon)} \quad \ldots (7)$$

Gk represents the generation of turbulence kinetic energy due to the mean velocity gradients. Gb is the generation of turbulence kinetic energy due to buoyancy. YM represents the contribution of the fluctuating dilatation in compressible turbulence to the overall dissipation rate. C_2 and $C_{1\varepsilon}$ are constants. σ_k and σ_ε are the turbulent Prandtl numbers for k and ε, respectively. $S_k$and Sε are user-defined source terms.

The difference between the realizable k-ε model and the standard k-ε and RNG k-ε models is that Cμ is no longer constant. Schnerr and Sauer Model has been used in numerical simulations. The vapor mass fraction, α, is governed by a transport equation

$$\frac{\partial}{\partial t}(\alpha\rho_v) + \nabla.(\alpha\rho_v \vec{V}_v) = R_e - R_c \quad \ldots (8)$$

The source terms Re and Rc denote vapour generation evaporation and condensation rates, and can be functions of flow parameters (pressure, flow character or velocity) and fluid properties (liquid and vapour phase densities, saturation pressure, and liquid vapour surface tension), Vv is the vapour phase density, α is the vapor phase volume and ρv is the vapor density. The results reported in this paper are achieved when the residuals are less than 1.0 x 10^{-2}.

C. Assumptions used in fluid flow modeling.

The important assumption for this one-fluid cavitation models that the mixture of liquid and vapor is homogenous, barotropic with no heat conductivity. This is the usual and realistic assumption for simulating cavitation occurring in cold water and under high pressure condition where the thermal effect and viscous loss are usually very much smaller than the mechanical (pressure) driving force of the system [8].

IV. RESULT AND DISCUSSION

A. Cone cavitator

From the fig 3.1 a-b, it is noticed that pressure rise on cone is as high a 26 bar at the tip of the nose. The entire cavitator nose is in contact with water, (fig 3.2 a-b), giving it maneuverability over the body, but comes at cost of material wear of the cone. The cavitation no. is around 0.16 in the cavity region formed behind the cone (fig 3.3 a-b).

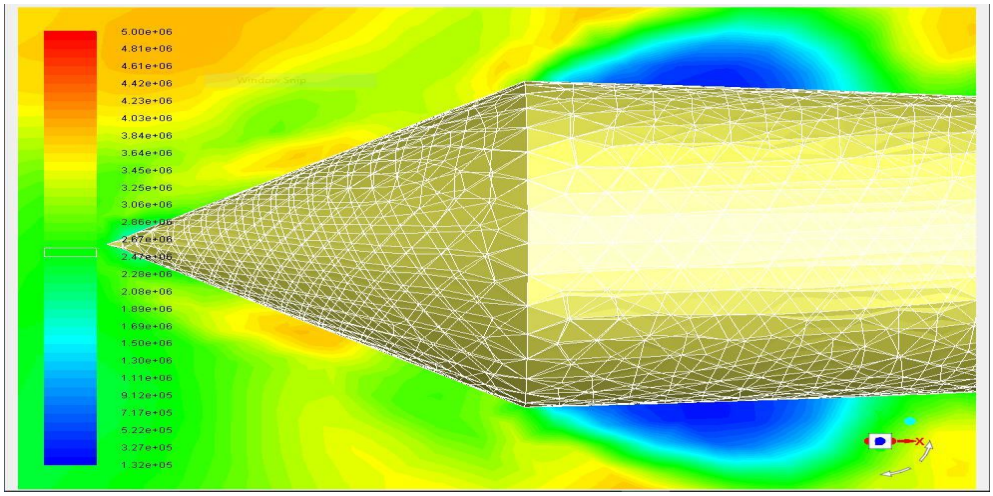

Fig: 3.1. a Pressure distribution of cone with aerodynamic body moving at 100m/s.

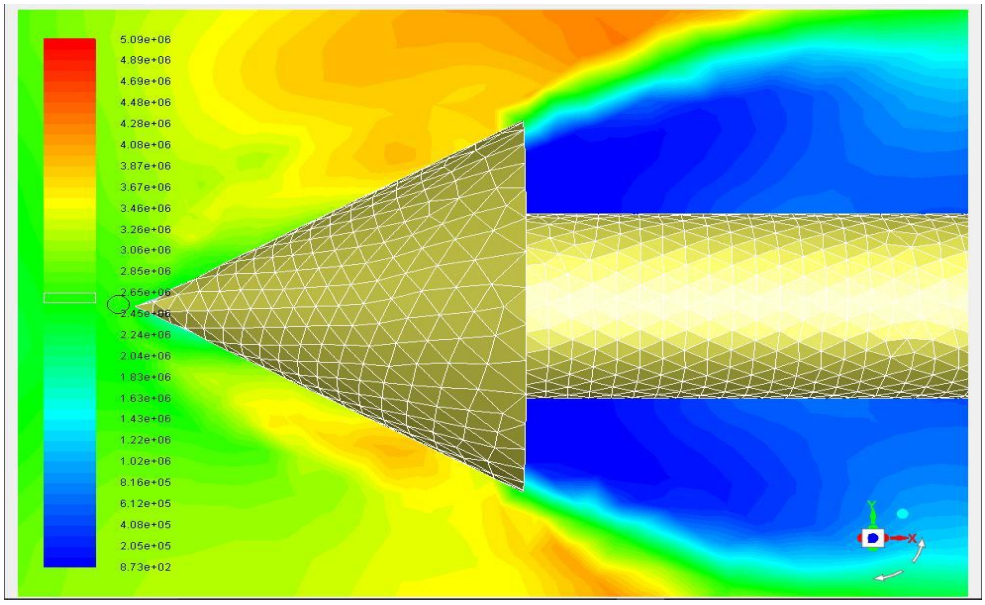

Fig: 3.1.b Pressure distribution of cone with cylinder moving at 100m/s.

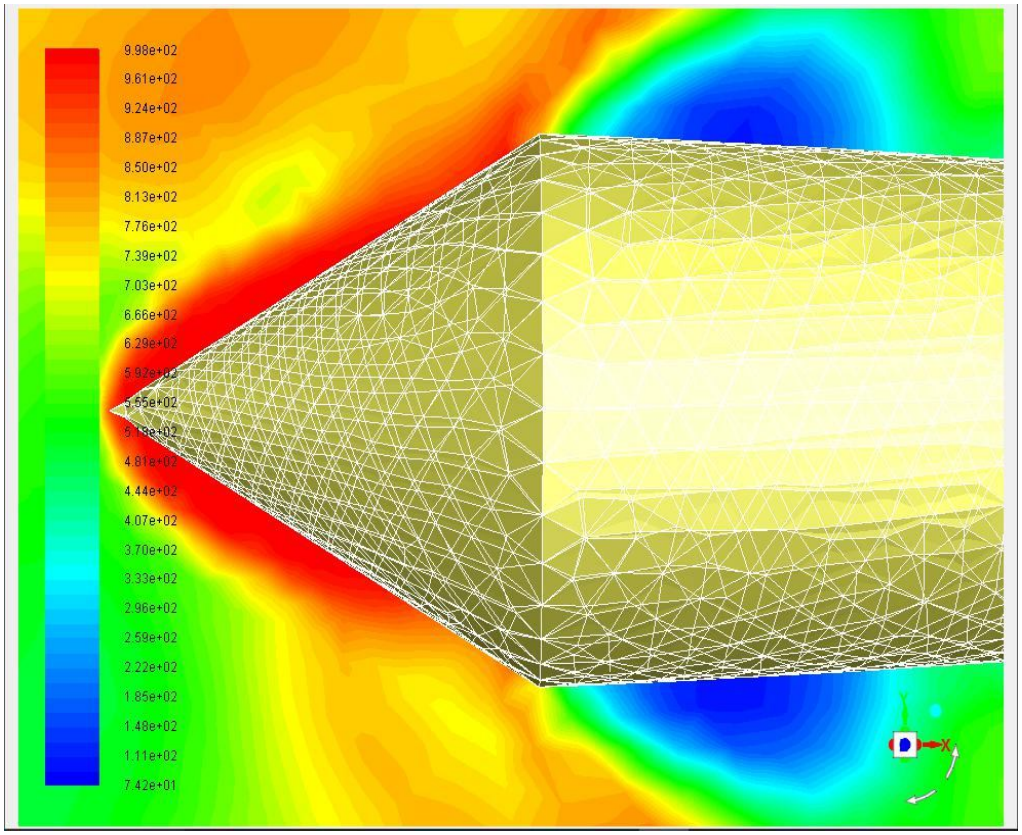

Fig: 3.2.a. Density distribution of cone head with aerodynamic body moving at 100m/s.

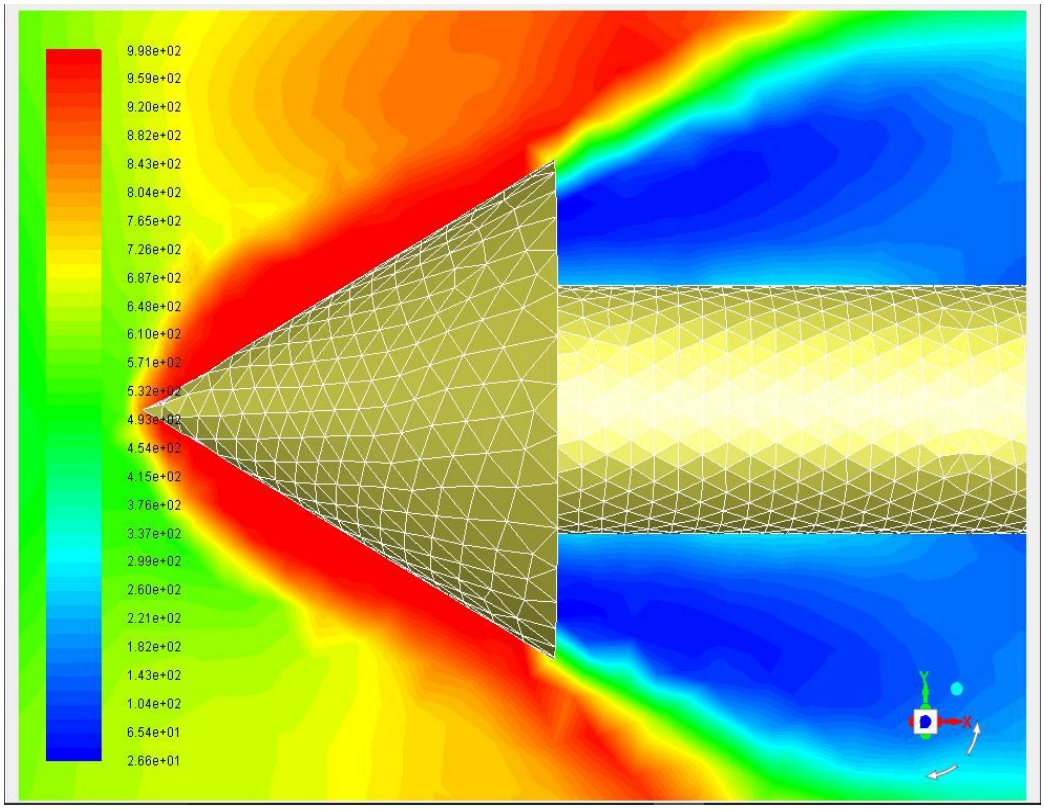

Fig: 3.2.b. Density distribution of cone head with cylinder body moving at 100m/s.

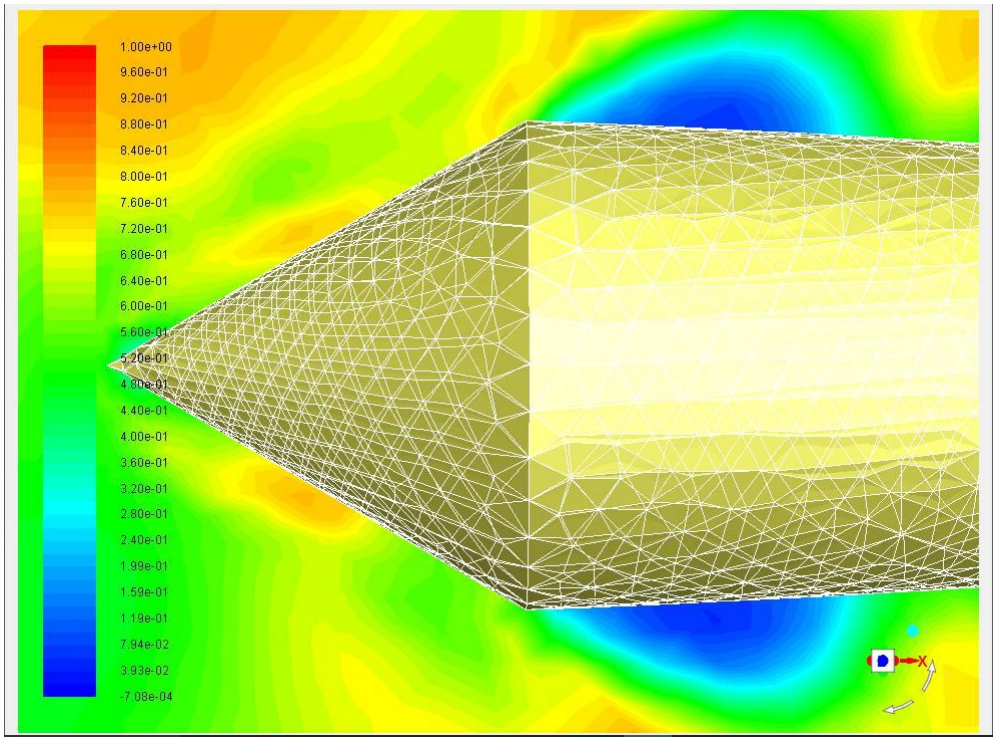

Fig:3.3.a Cavitation no. profile of cone head with aerodynamic body moving at 100m/s.

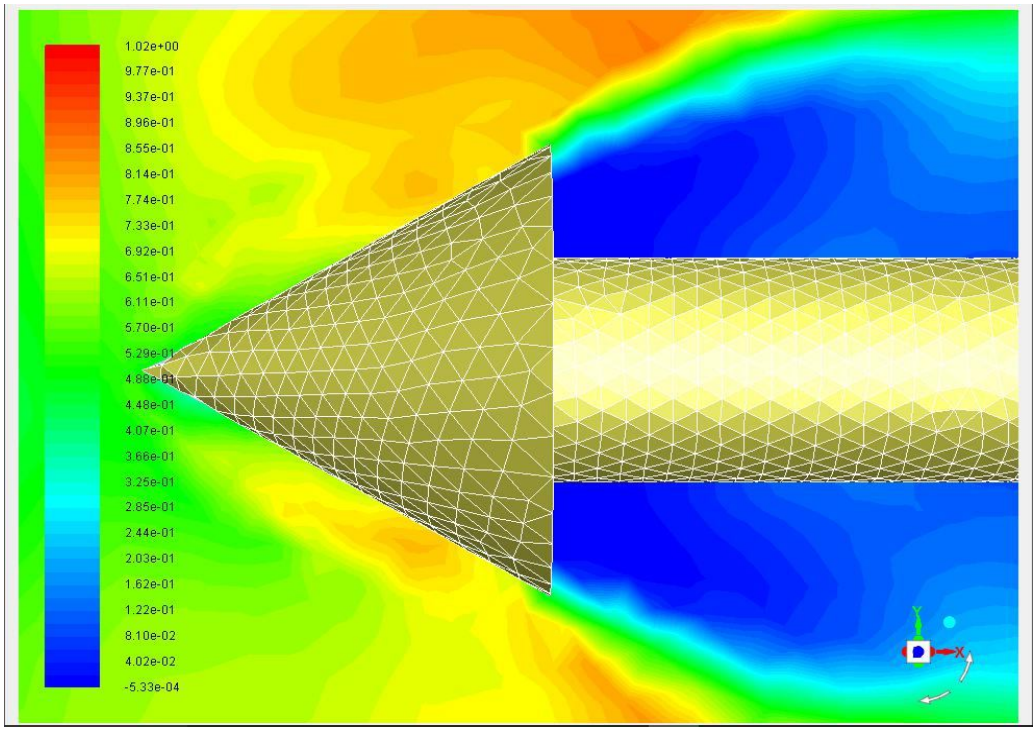

Fig: 3.3.4 Cavitation no. profile of cone head with cylinder body moving at 100m/s.

B. Hemi-spherical cavitator.

From the fig 4.1a-b, it is noticed that pressure rise on hemisphere is only a 2 bar at the tip of the nose. The entire cavitator nose is in contact with water and has greater contact area than cone head, (fig 4.2 a-b), giving it better maneuverability over the body, but

comes at cost of material wear of the hemispherical head. The cavitation no. is around 0.10 in the cavity region formed behind the cone (fig 4.3a-b).

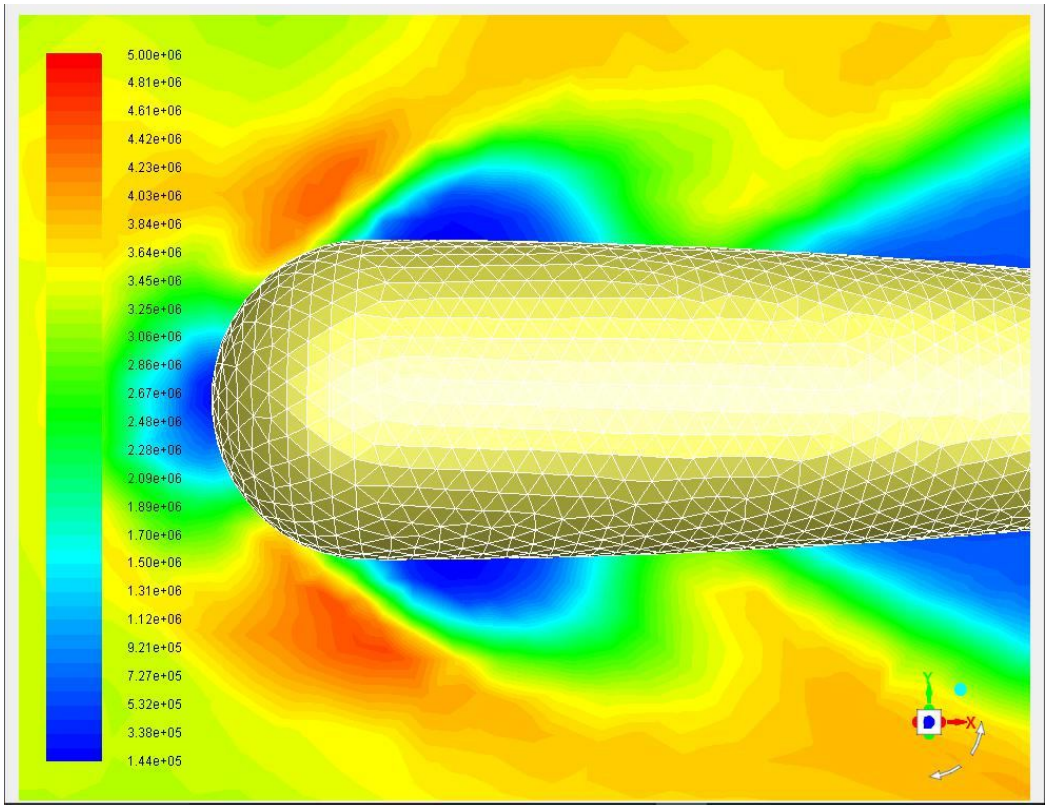

Fig: 4.1.aPressure distribution of hemispherical head with aerodynamic body moving at 100m/s.

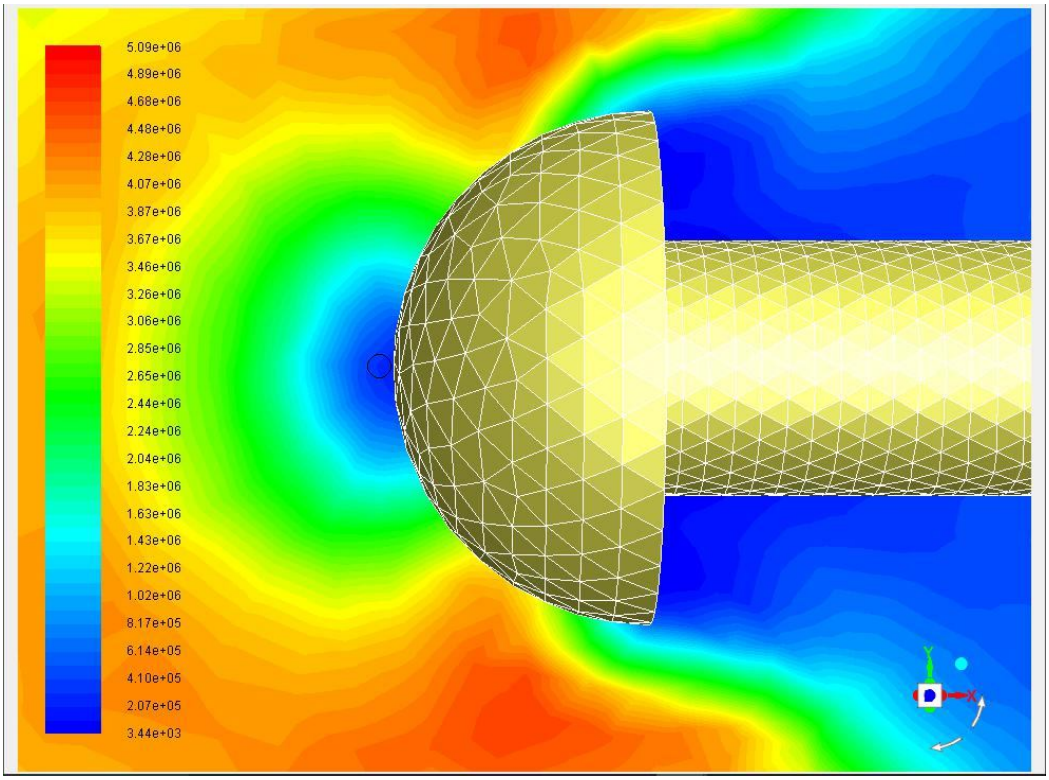

Fig: 4.1.b Pressure distribution of hemispherical head with cylinder moving at 100m/s.

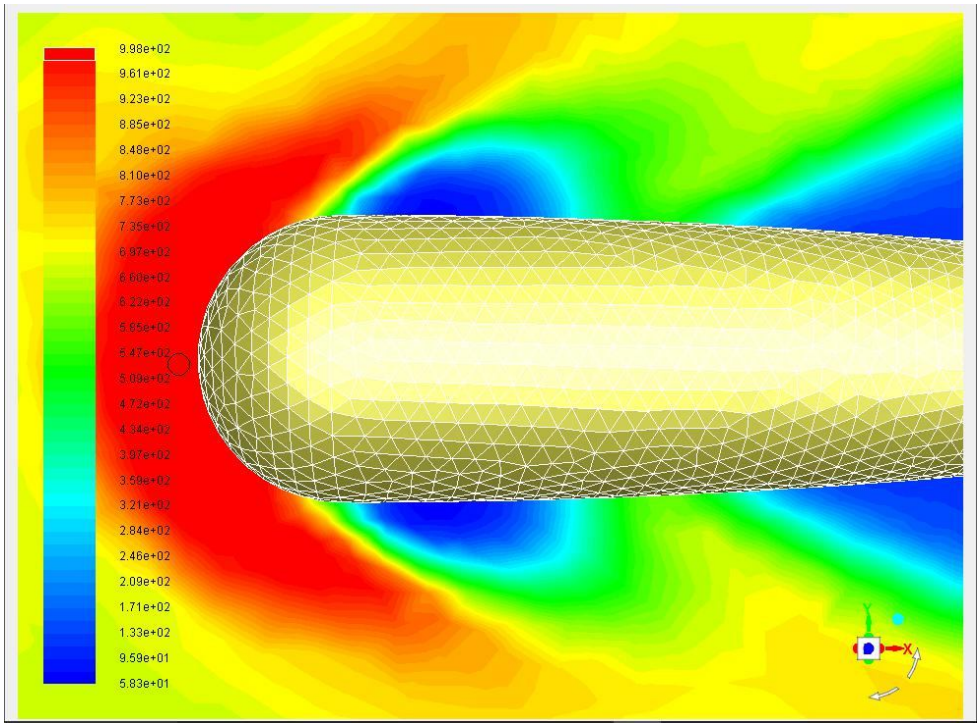

Fig: 4.2.a. Density distribution of hemispherical head with aerodynamic body moving at 100m/s.

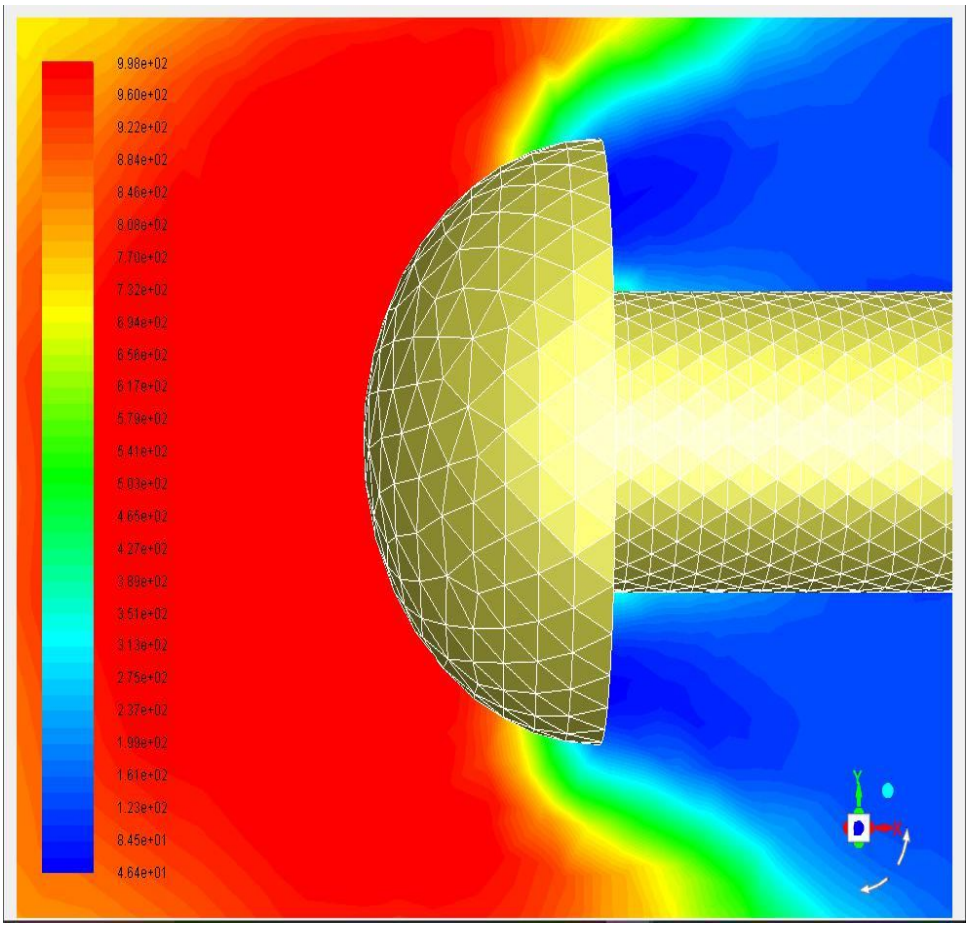

Fig: 4.2.b. Density distribution of hemispherical head with cylinder body moving at 100m/s.

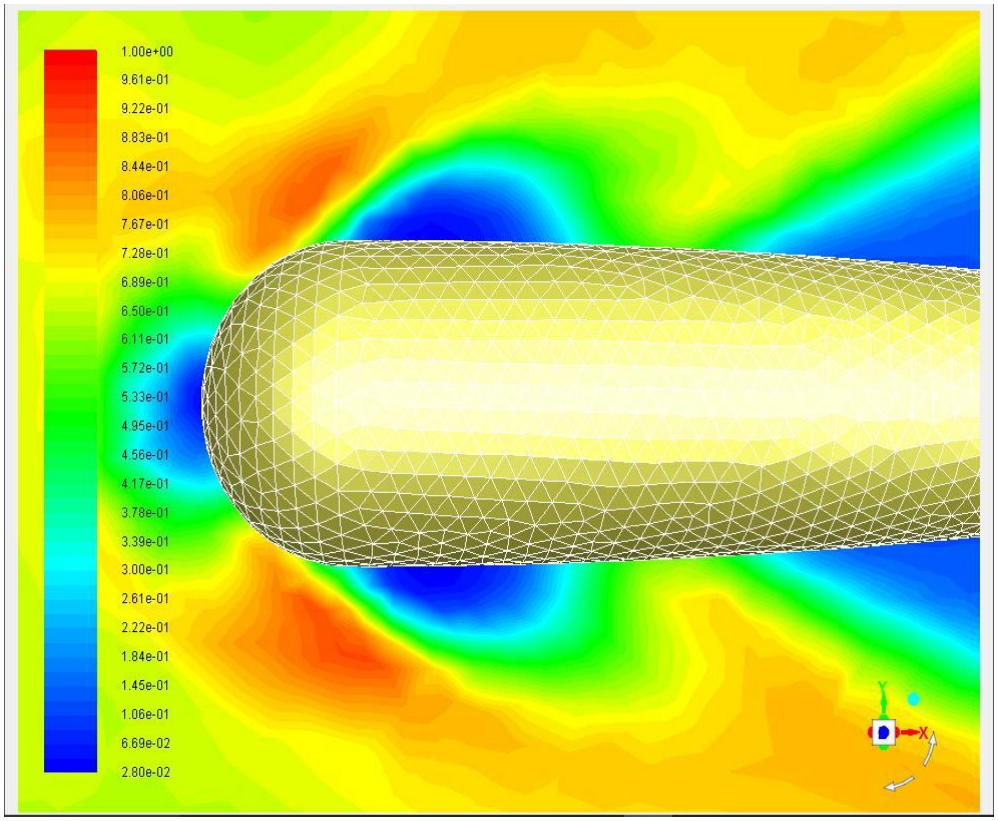

Fig: 4.3.a Cavitation no. profile of hemispherical head with aerodynamic body moving at 100m/s.

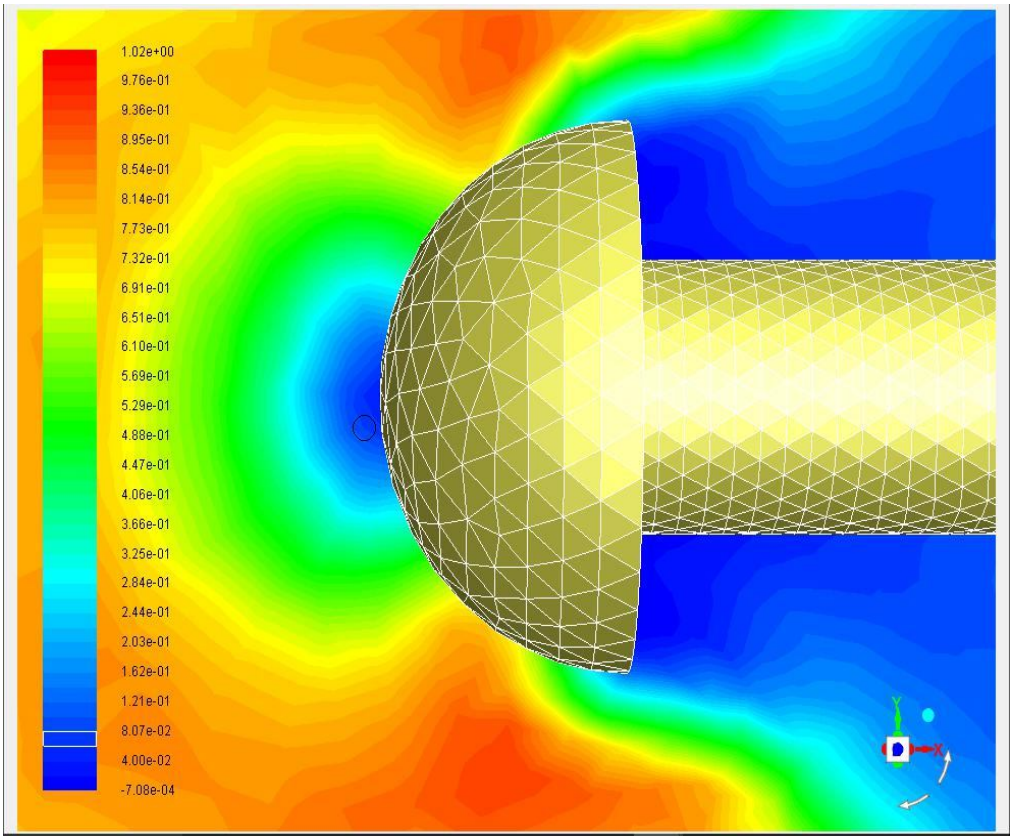

Fig: 4.3.b Cavitation no. profile of hemispherical head with cylinder body moving at 100m/s.

C. Cylinder and aerodynamic body

The pressure distribution is more gradual for aerodynamic body and irregular for cylinder body (fig 5.1a-b). The cylinder body experiences a sudden collapse in the cavity near the middle region, fig 5.2b, however, in the cave of aerodynamic body the cavity is stable and collapses some distance after the tail end, fig 5.3 b.

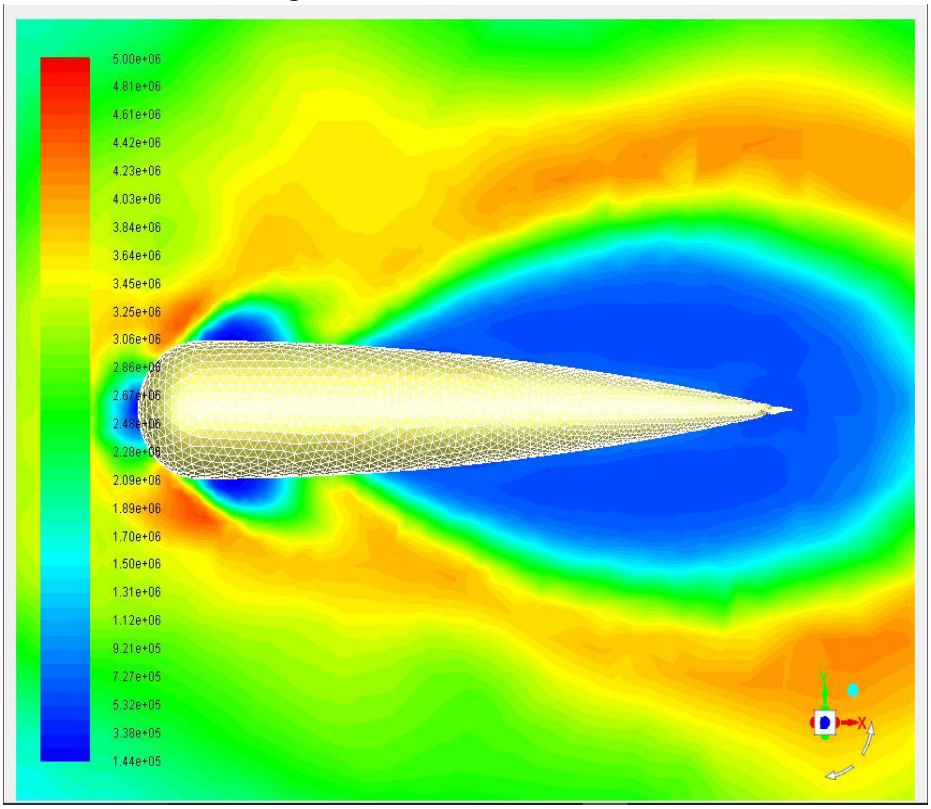

Fig: 5.1a Pressure distribution of hemispherical head with aerodynamic body moving at 100m/s.

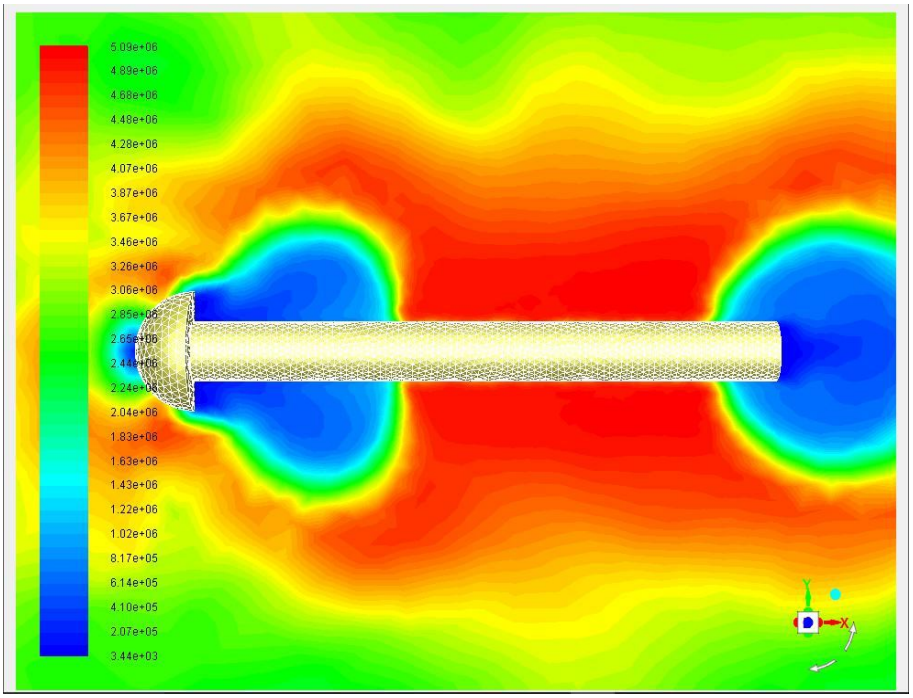

. Fig: 5.1b Pressure distribution of hemispherical head with cylinder moving at 100m/s.

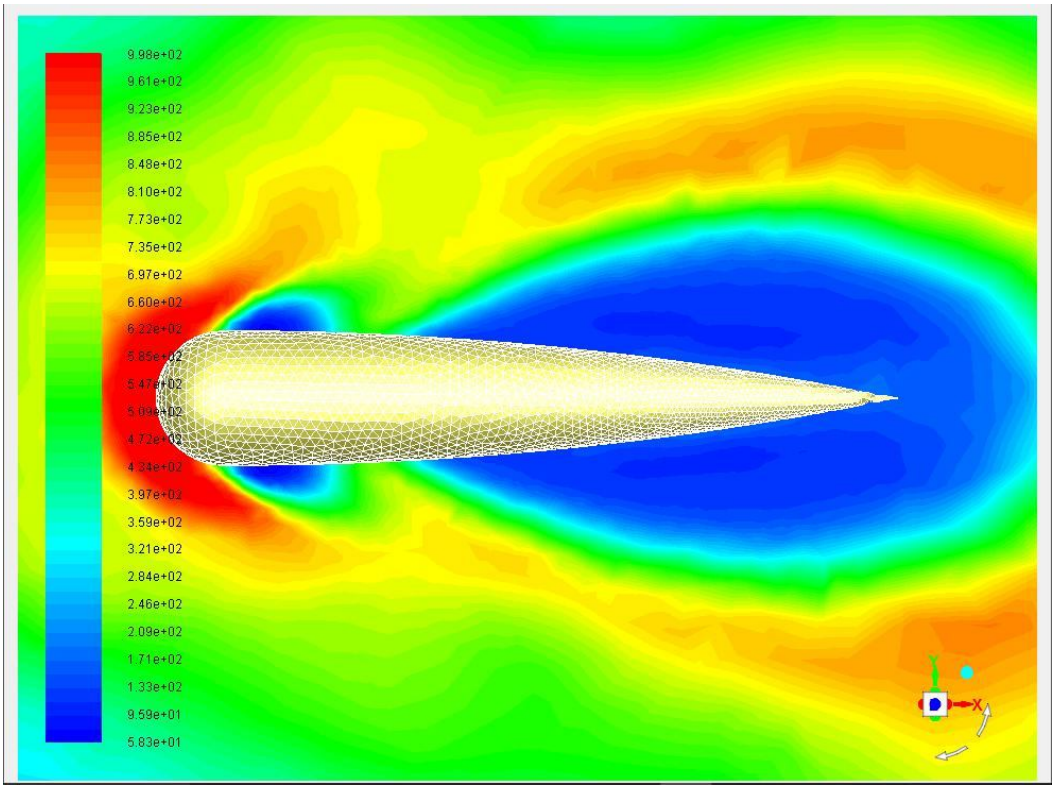

Fig: 5.2a. Density distribution of hemispherical head with aerodynamic body moving at 100m/s.

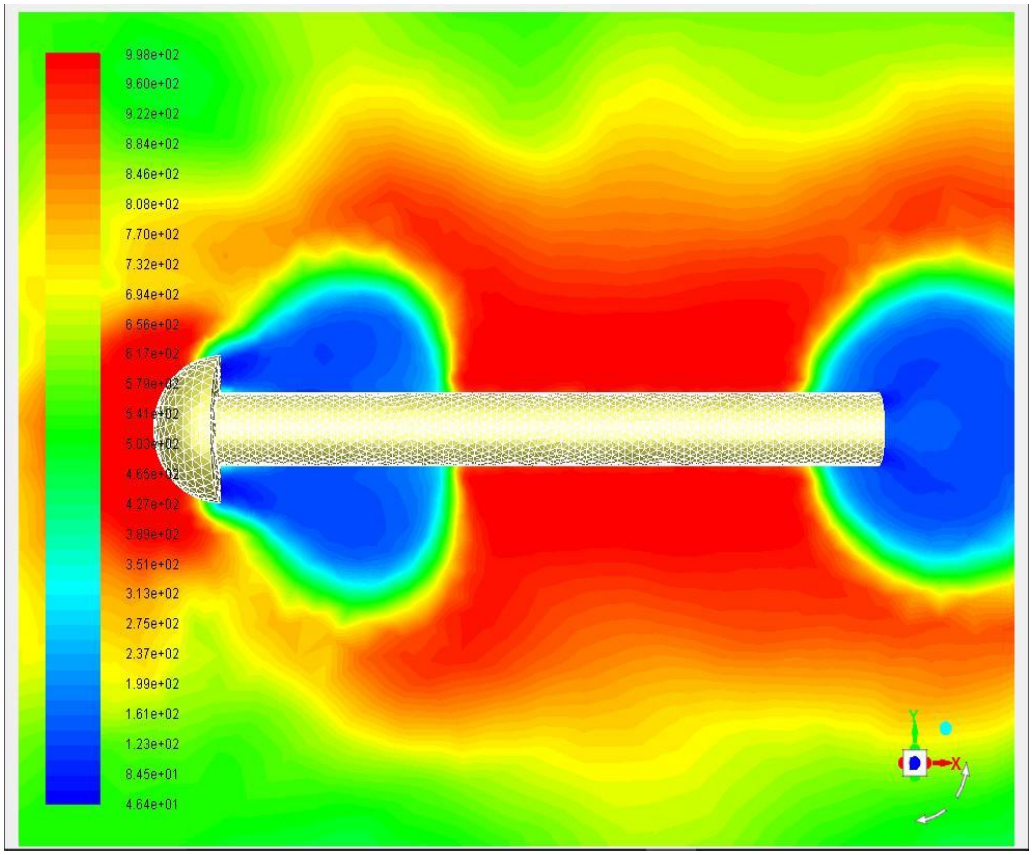

Fig: 5.2b. Density distribution of hemispherical head with cylinder body moving at 100m/s.

ISSN: 2321-9653; IC Value: 45.98; SJ Impact Factor:6.887
Volume 6 Issue I, January 2018- Available at www.ijraset.com

V.CONCLUSIONS

In this paper the numerical investigation of important unsteady supercavitation features is presented. The URANS dynamics model is used as numerical method in order to simulate unsteady supercavitation shape and informative feature of unsteady supercavitation phenomenon. It is discovered that aerodynamic model produces gradual pressure distribution at high speed as compared to cylinder body. The hemispherical head is a viable choice for body design due to it lower pressure rise at the tip and also gives better manoeuvrability having more region in contact with water.Finally, the results produced in this report will help in design and optimization of underwater AUVs (Autonomous Underwater Vehicles) moving at high speeds.

VI. ACKNOWLEDGMENT

I would first like to thank my advisor Dr. Anand Raj Hariharan of the ASIET . He consistently allowed this paper to be my own work, but steered me in the right the direction whenever he though I needed it.

REFERENCES

[1] Suprcavitation Research and Development
[2] Ivan N. Kirschner, Neal E. Fine, James S. Uhlman, David C. Kring, and Benjamin J. Rosenthal
[3] Natural Supercavitation Characteristic Simulation of Small-caliber Projectile, PAN Shou-li, ZHOU Qiang, 2014
[4] ANSYS Documentation and ANSYS Help 17.0
[5] Numerical Simulation of Supercavitation, ZengHuiming, 2007
[6] High-speed imaging of supercavitation projectiles. J D Hrubes, 2001
[7] Rouse, H. &McNown, J.S., Cavitation and Pressure distribution: head forms at zero angle of yaw, State University of Iowa, Studies in Engineering Bulletin 32, 1948.
[8] Vlasenko, Y.D., Experimental investigation of supercavitation flow regimes at subsonic and transonic speeds. Proc. 5th Int. Symp. On cavitation (Cav2003), Osaka, Japan, 2003.
[9] Owis, F.M. &Nayfeh, A.H., Computations of the Compressible Multiphase Flow over the Cavitating High-Speed Torpedo, Journal of Fluids Engineering, 125, pp.459-468, 2003.
[10] Klomfass, A. & Salk, M., Numerical analysis of the supercavitating supersonic flow about blunt bodies, 25th International Symposium on Shock Waves (ISSW25), 17-22 July, Bangalore, India, 2005.
[11] Neaves, M.D. & Edwards, J.R., All-speed time-accurate underwater projectile calculations using a preconditioning algorithm, Journal of Fluids Engineering, 128(2), pp.284-296, 2006.
[12] Experimental and numerical investigation of an unsteady supercavitating moving body, B. Saranjam, 2013

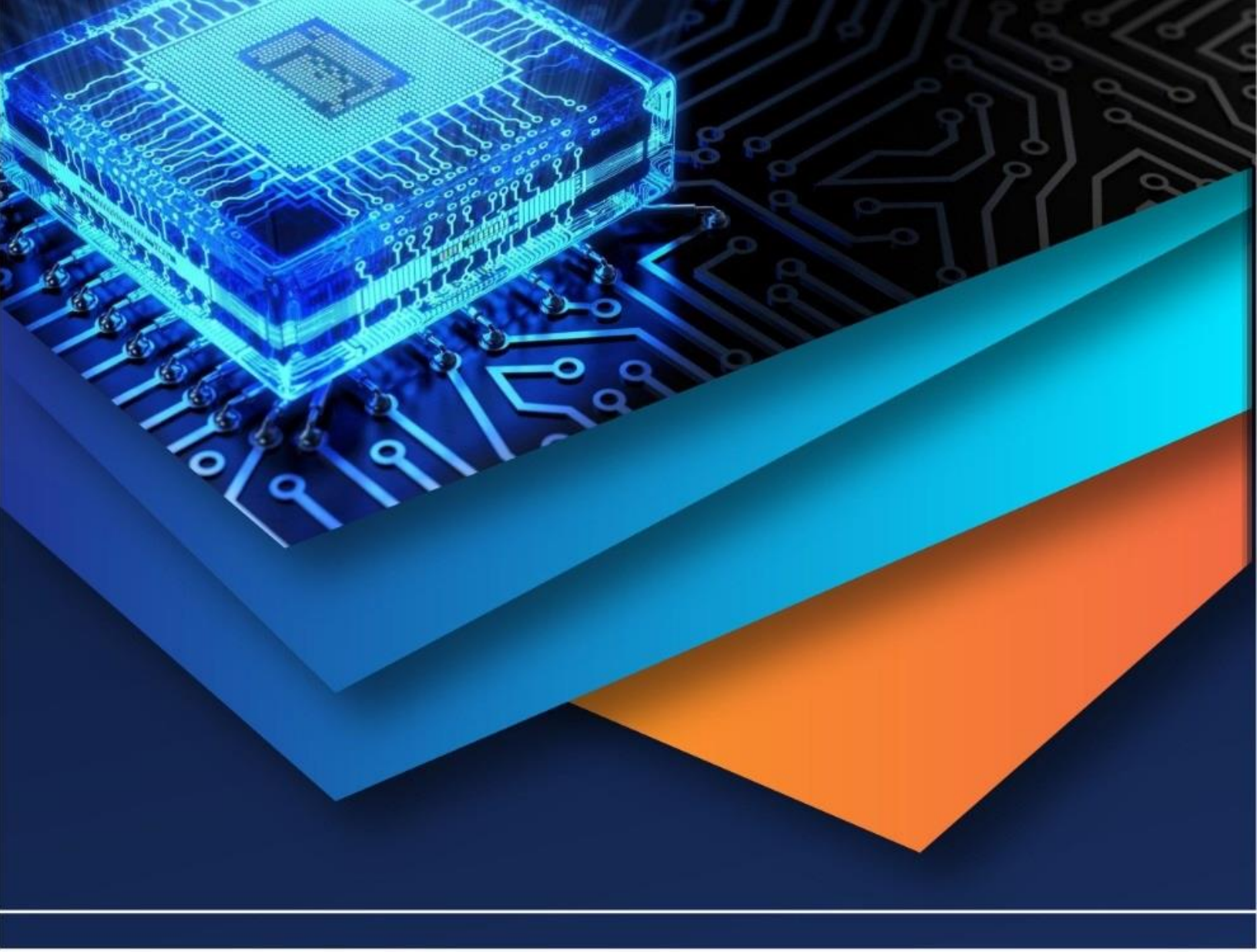

10.22214/IJRASET

45.98

IMPACT FACTOR: 7.129

IMPACT FACTOR: 7.429

INTERNATIONAL JOURNAL FOR RESEARCH

IN APPLIED SCIENCE & ENGINEERING TECHNOLOGY